

Effect of Reactor Model Modifications on the Sensitivity and Uncertainty of K_{eff} and Reactivity

Mohga Hassan, Basma Foad²

^{1,2}Egypt Nuclear and Radiological Regulatory Authority, 3 Ahmad El Zomar St., Nasr City, Cairo, 11787, Egypt
¹mohgaig[at]yahoo.com

Abstract: In nuclear reactor physics models, a major source of uncertainty is cross sections uncertainties, which is dependent upon model specifications. The main objective of this work is to study the effect of change in some reactor model details on the sensitivity and uncertainty of k_{eff} and reactivity. Modifications considered for k_{eff} sensitivity and uncertainty estimations are change in coolant density and burnable absorber design. Reactivity sensitivity and uncertainty is affected by control rod design modification. The KSEN card of MCNP6 code is used to calculate the sensitivity vectors for ^{235}U , ^{238}U , and ^1H , in two PWR cores with differences in design. NJOY2021 was used to compute the relative covariance matrices of the cross-sections data library. A python script was developed to read the MCNP and NJOY outputs, and to calculate the uncertainties of k_{eff} as well as sensitivities and uncertainties of reactivity due to the control rods insertion.

Keywords: Sensitivity, Uncertainty, NJOY, MCNP6

1. Introduction

In any reactor simulation model, uncertainties necessarily exist. In case of reactor physics the major source of uncertainty comes from cross section uncertainties which depends on problem formulation, including materials, geometry, temperature, ...etc.

The uncertainty propagation methods can be classified into two approaches [1,2]. The first is the Monte Carlo based technique (statistical sampling method), which starts by calculating uncertainty by randomly generating possible inputs, then analyzing the distribution of outputs generated by randomly varying inputs. The sampling-based uncertainty is relatively simple but it is computationally expensive since it needs to run N-times, where N is the sample size. It also has the statistical error which varies as inverse square root with the sample size [3].

The second technique is the sensitivity based technique [1,2] (deterministic method), it includes two methodologies, the forward (direct) calculation method implemented by varying the inputs one by one and observing the responses, this approach is preferable when there are few input parameters that can vary and many output responses of interest.

The second deterministic method is the adjoint method based on the perturbation theory, in which the sensitivity is calculated using adjoint functions. The perturbation theory will be used in the present work to calculate sensitivity coefficients.

The BEAVRS (Benchmark for Evaluation and Validation of Reactor Simulation) benchmark problem provides detailed specification of the geometries and compositions for the commercial pressurized water reactor (PWR) core with 3411 MWth. The main purpose of BEAVRS is to allow various reactor physics computer codes to construct the neutronic calculation model of the full-core with real plant data, and it was modified several times [4-6]. In this work we are interested in modification from version1 (henceforth BV1)

[4], to the last version (henceforth BV2) [6]. Modifications include coolant temperature and densities in the nozzle and support plate structure, the designs of the burnable absorber rod, and the control rods, in addition to some modifications in the upper and lower structures. In this paper the effect of the above mentioned design changes on the sensitivity coefficients of multiplication factor are investigated. Reactivity sensitivity and uncertainty resulting from control rod design change are also evaluated.

MCNP6.1[7] is used to calculate sensitivity coefficients. MCNP6.1 offers two perturbation theory techniques: one is based on the differential operator (PERT card) and another is based on linear perturbation theory using adjoint weighting (KPERT and KSEN cards). Both methods have advantages and disadvantages. The differential operator technique is based on a Taylor series expansion and works very well for generalized responses with fixed-source problems. In eigenvalue problems, however the differential operator methodology may produce inaccurate results, because MCNP6 implementation does not account for the perturbation of the fission source distribution. The adjoint weighting perturbation methodology invoked by KPERT card was designed to investigate changes in k_{eff} as a result of material substitution. While the method, in theory, allows for more general perturbations, it introduces an approximation in the handling of scattering laws that can lead to large and unacceptable deviations in scattering sensitivities. For this reason, the KSEN capability, that is more accurate and efficient and easier to use than KPERT for this purpose, has been developed. In this paper, KSEN card is used for calculating MCNP6 sensitivity coefficients [8].

The paper is organized as follows: the next section explains the theory and mathematical model used in this study. Section 3 summarizes the differences between BV1 and BV2 models. In Section 4, the MCNP6 model, used to simulate both models and calculate the sensitivity coefficients, is explained. Section 5 illustrates the calculation steps and the relation between MCNP6,

NJOY[9], and the python module. In Section 6, the sensitivity and uncertainty analyses for both models are presented, finally, the conclusion is summarized in Section 7.

2. Theory

As mentioned above, we will use adjoint method based on the perturbation theory, in which the sensitivity is calculated using adjoint functions.

2.1 Sensitivity of k_{eff}

In general, the sensitivity coefficient is defined by the relative change of the core characteristic, due to the relative change of the cross-section:

$$S(R) = \frac{dR/R}{d\sigma/\sigma} \quad (1)$$

where R is the core characteristics, such as k_{eff} , and σ is the cross-section.

In this work KSEN card of MCNP6 code, which is based on adjoint weighting, is used to estimate sensitivity coefficients. Details of the modeling basis and usage of this function can be found in the references [7,8].

2.2 Sensitivity of reactivity

The reactivity associated with the change in conditions (control rod insertion, temperature, coolant, density, etc.) is defined as:

$$\rho_{1 \rightarrow 2} = \rho_2 - \rho_1 = \frac{1}{k_{eff1}} - \frac{1}{k_{eff2}} \quad (2)$$

$$\sigma_{\rho}^2 = \left(\frac{1}{|\rho_{1 \rightarrow 2}|} \right)^2 \sigma_{k_{eff1}}^2 + \left(\frac{1}{|\rho_{1 \rightarrow 2}|} \right)^2 \sigma_{k_{eff2}}^2 - \left(\frac{\frac{1}{k_{eff1}k_{eff2}}}{\left(\frac{1}{k_{eff1}} - \frac{1}{k_{eff2}} \right)^2} \right) \sigma_{k_{eff1},k_{eff2}}^2 \quad (6)$$

Where $\sigma_{k_{eff1}}^2$ and $\sigma_{k_{eff2}}^2$ are the relative variance of the k-eigenvalues, and $\sigma_{k_{eff1},k_{eff2}}^2$ is the relative covariance of the two eigenvalues.

3. Core Modifications

There are major differences between BV1 and BV2 cores, which include modifications in the core model which will affect the multiplication factor when all control rods are out of the core. In addition, there are changes in the control rod design that will impact the reactivity coefficients due to control rods insertion. Here are the major updates between the BV1 and BV2 cores that are considered in the present study, other detailed data can be found in the reference [4-6]:

- The coolant in the nozzle and support plate structures have different temperatures and densities from that in the core. In the BV1 core, the coolant temperature and density were set to 566.5 °K and 740.6 kg/m³, respectively. While

Where k_{eff1} and k_{eff2} are the k-eigenvalues for two different states. In this study, the case where all control rods are out represents state-1 and all control rods in represents state-2.

Williams in reference [10] gave a detailed description of the sensitivity methodology for reactivity responses. He proved that the reactivity sensitivity coefficient, due to change of any arbitrary parameter α , is equal to

$$S_{\alpha}(\rho) = \frac{\lambda_2 S_{k_2,\alpha} - \lambda_1 S_{k_1,\alpha}}{|\rho_{1 \rightarrow 2}|} \quad (3)$$

Where λ_1, λ_2 equals $\frac{1}{k_1}$ and $\frac{1}{k_2}$ are the fundamental lambda Eigenvalues before and after the change, and $S_{k_1,\alpha}, S_{k_2,\alpha}$ are the k-sensitivities for the two states, and $|\rho_{1 \rightarrow 2}|$ is the absolute value of reactivity change. For isotope i reaction j and energy group g the sensitivity of reactivity is given by:

$$S_{i,j,g}(\rho) = \frac{\frac{1}{k_{eff2}} S_{i,j,g}(k_{eff2}) - \frac{1}{k_{eff1}} S_{i,j,g}(k_{eff1})}{|\rho_{1 \rightarrow 2}|} \quad (4)$$

2.3 Uncertainty calculation method

The sandwich formula is used to calculate the uncertainty or the relative variance of core response 'R'; given by [1,10]:

$$var(R) = \sigma_R^2 = S(R) \cdot C \cdot S^T(R) \quad (5)$$

where S(R) is the sensitivity vector which includes all reactions, nuclides, and energy-groups, the subscript 'T' denotes transpose, and 'C' is the relative covariance matrix describing cross-section uncertainties and correlations, which are computed using the NJOY2021 code [5]. The relation between the uncertainties of the k-eigenvalues and reactivity responses was investigated in reference [10] as follow:

in the BV2, the coolant temperature and density in the nozzle and support plate were updated to 349.1 °K and 981.0 kg/m³ °K, respectively.

- The part under the bottom of the burnable absorber rod in BV1 was water in the lower part of the guide tube, while in BV2, the bottom part of the absorber rod is stainless steel (SS) pin introduced as an end plug.
- The control rod material was only Silver Indium Cadmium (Ag-In-Cd) in BV1. In BV2, the control rods are divided into two parts, an upper part of about 259 cm has boron carbide (B₄C) as an absorber, while the lower part of about 102 cm has Ag-In-Cd absorber.

4. Calculation Steps

The overall calculation steps are schematically summarized in Figure 1, and detailed in the following:

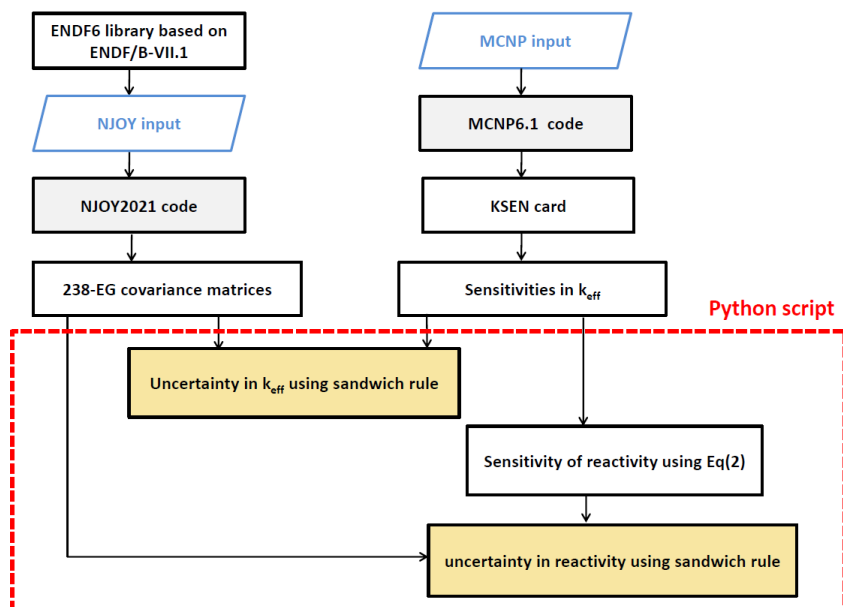


Figure 2: Flowchart for the calculation steps

- Two full core models were prepared using the MCNP6.1 code [7]. A 238-energy group structure was used in calculating the sensitivity coefficient, from a minimum of 1×10^{-10} to 20 MeV. The calculations were performed using 175 million neutron histories; 500,000 neutron per cycle, 150 skipped cycles, and 350 active cycles.
- Multiple runs for the two cores were performed utilizing KSEN card, with all rods out then all rods in. The sensitivity and uncertainty (S&U) were estimated with all control rods out to evaluate the effect of using different coolant temperatures and densities in the nozzle and support plate structures in addition to the impact of changing the control rods design. The influence of changing the control rods design is investigated by studying the S&U of reactivities resulting from control rods insertions. Cross sections considered in this study are listed in table 1.

Table 1: Cross Sections Considered in the study

Nuclide	Cross Section
^1H	$\sigma_c \sigma_e$
$^{235}\text{U}, ^{238}\text{U}$	$\sigma_f, \sigma_c, \sigma_e, \sigma_{ine}, \text{fission-}\nu, \text{fission-}\gamma$

- Then, the NJOY2021 code [9] is used to compute the covariance matrices of the ENDF/B-VII.1 cross-section data library[11].

- Thereafter, a python program is developed to read the k_{eff} sensitivity coefficients calculated by the KSEN card of MCNP6 code, and also read the covariance matrices generated by the NJOY2021 code.
- The python script uses the sandwich rule (Eq.(5)) to compute the uncertainties in k_{eff} .
- Then, the sensitivity of reactivity coefficients resulted from the perturbations caused by insertion of control rods are calculated using Eq.(4) for the two cores.
- Finally, the uncertainties in reactivity coefficients are calculated using the sandwich formula (Eq.(5)).

5. Results and Discussion

5.1 Sensitivities and Uncertainties in k_{eff}

Figures 2 to 4 shows the result of sensitivity coefficient produced by KSEN card of MCNP6. These sensitivities are for all rods out where the dominating factor is the change in water density. The case of all rods in will be mostly affected by the change in control rod design; so it will only be discussed in integrated reactivity of k_{eff} and in reactivity sensitivity. From figures 2 to 4 we can see that the most affected sensitivity profiles are σ_e for all isotopes in this study, and σ_{ine} , and fission- γ , for ^{235}U and ^{238}U .

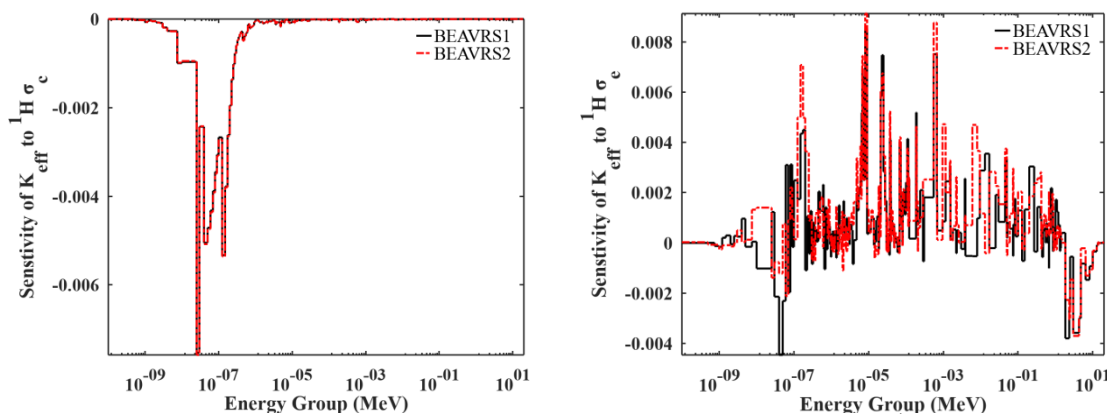


Figure 2: Sensitivity Coefficients of K_{eff} – Control Rods Out ^1H

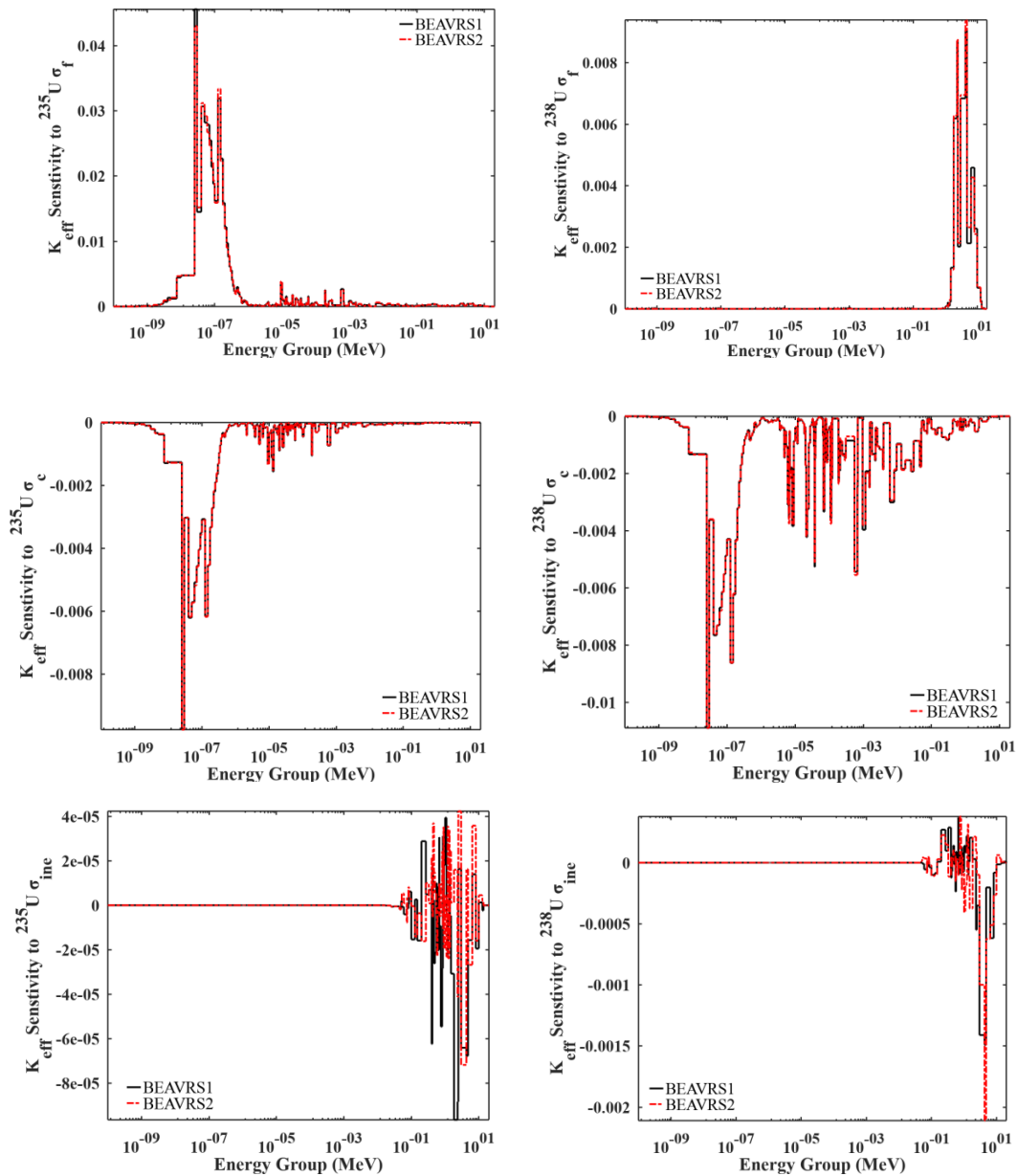
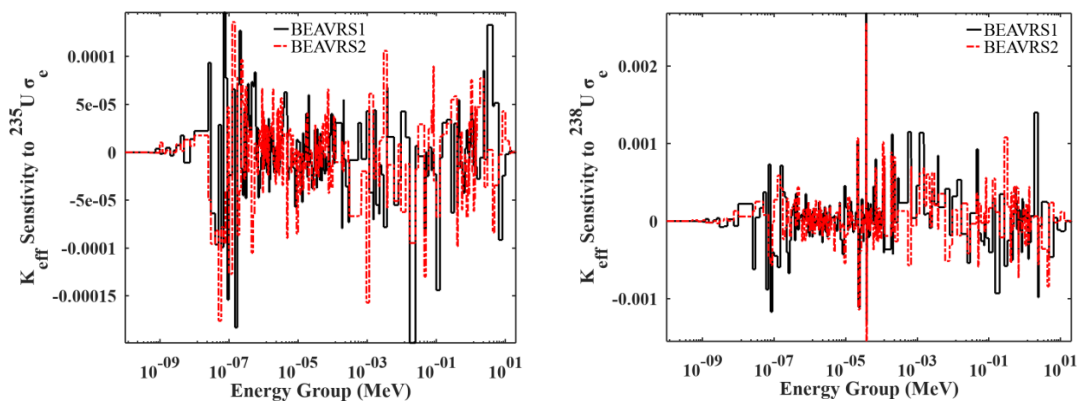


Figure 3: Sensitivity Coefficients of K_{eff} – Control Rods Out ($\sigma_f, \sigma_c, \sigma_{ine}$ for $^{235}\text{U}, ^{238}\text{U}$)



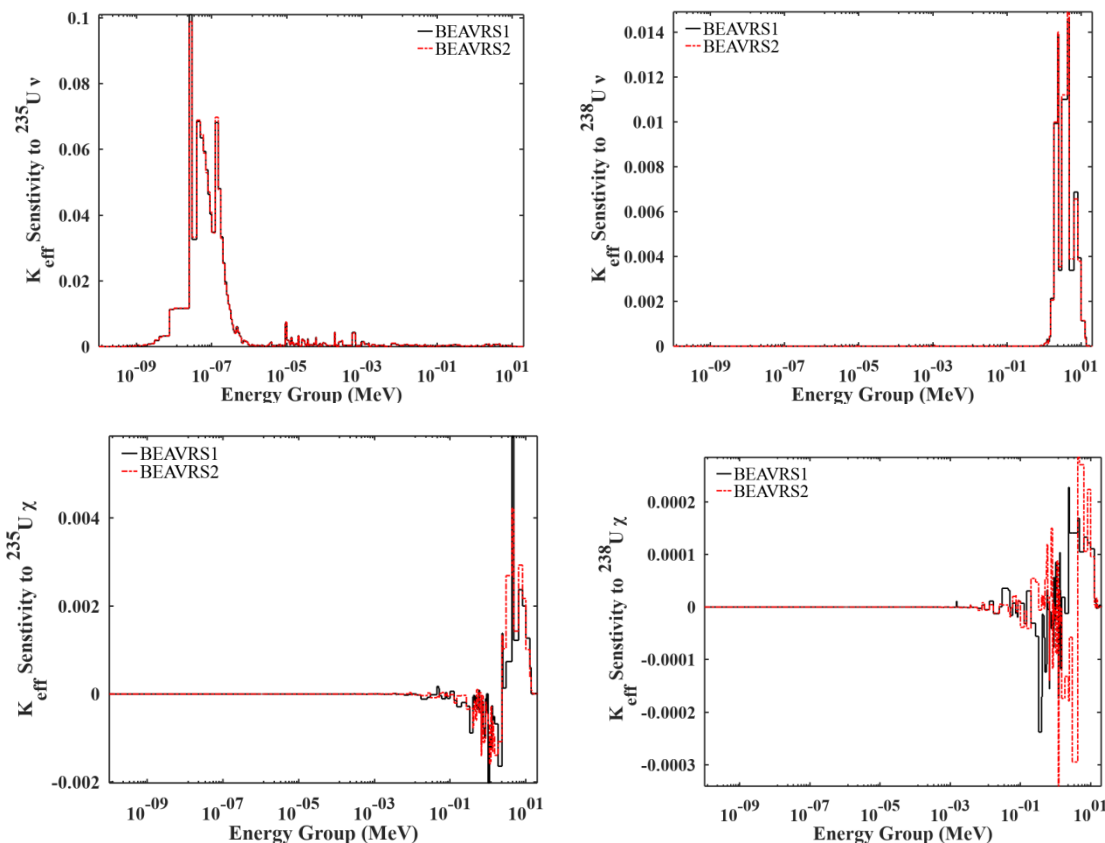


Figure 4: Sensitivity Coefficients of K_{eff} – Control Rods Out (σ_e , fission- v , fission- γ for ^{235}U , ^{238}U)

Figure 5 shows the energy integrated sensitivity coefficients in k_{eff} due to perturbations in cross-sections for BV1 and BV2 when all control rods are in and out.

As can be seen in Figure 5, the multiplication factor is very sensitive to ^{235}U fission- v and fission cross-sections, where sensitivities are positive, which means that k_{eff} increases as fission- v and fission cross-sections increase. The multiplication factor is also sensitive to ^{238}U capture cross-section, sensitivities that have negative values indicating that k_{eff} decreases as ^{238}U capture cross-section increases.

When all control rods are out, the differences between BV1 and BV2 sensitivities come from using different coolant densities in the nozzle and support plate structures and the effect of the changes in burnable absorber design. To explain these effects in more detail, let's look at the sensitivity profile of ^{235}U , ^{238}U when all control rods are out, as presented in Figures 3 and 4.

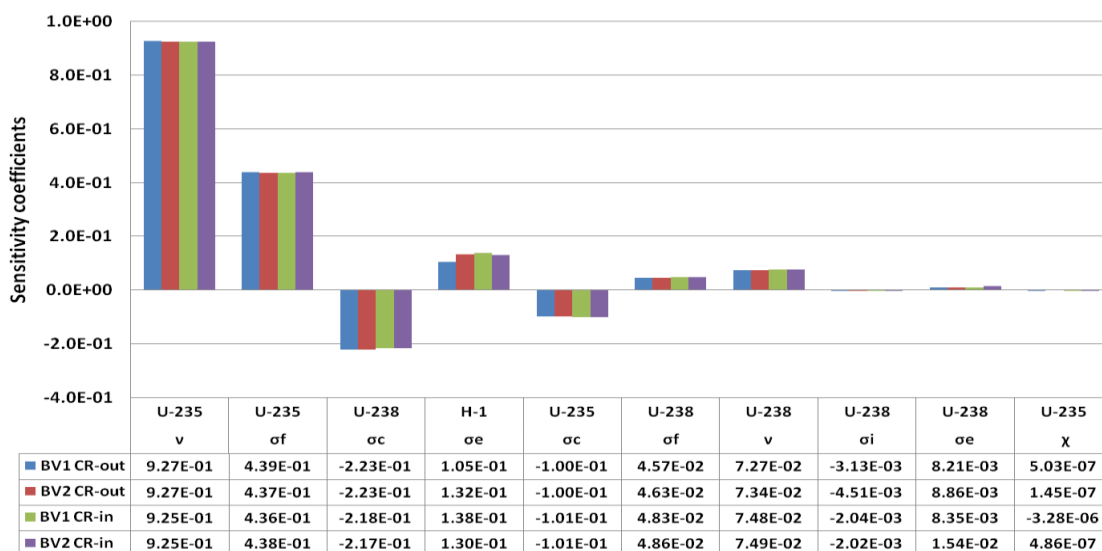


Figure 5: The integrated sensitivities in k_{eff} for BV1 and BV2

For the fission, fission- ν and capture, there are negligible differences between BV1 and BV2 sensitivities. The reason for that is the influence of modifications in the BV2 cores on the neutron spectrum. There are two main effects, the first effect is the higher coolant density in the nozzle and support plate structures of the BV2 model, which slightly increases the slowing-down process caused by water scattering cross-section, as a result, there will be a reduction on fast neutrons. The second effect is the burnable absorber design in the BV2 model, the water which filled the bottom part of the absorber rod (in BV1 model) is replaced by stainless steel, leading to an abundance of fast neutrons compared to the BV1 core, where the two effects work in opposite directions.

For the ^{238}U inelastic scattering, the k_{eff} sensitivities for some energy groups increase while others decrease causing an overall increment in the BV2 core integrated sensitivity.

For the ^{235}U fission- ν and ^{238}U capture, the two effects have negligible influences since the k_{eff} is more sensitive to thermal groups for both reactions, in addition, the sensitivity coefficients for the ^{235}U fission- ν and ^{238}U capture are high

and such small changes in the neutron spectrum is insignificant.

When all control rods are inserted into the core, the control rods worth strongly affects the neutron spectrum, such enormous effect overcomes the coolant density and the burnable absorber design effects that were mentioned before.

Figure 6 shows the total k_{eff} uncertainties and the significant contributors caused by cross-section uncertainty of individual nuclides for the BV1 and BV2 models when all control rods are in and out.

When all control rods are out, the total uncertainties for BV1 and BV2 models are 0.79 and 0.80 $\Delta k/k$ %, respectively. The total uncertainty slightly decreased to 0.78 $\Delta k/k$ % for both models when all control rods are in. The main contributors to the uncertainties are the ^{235}U fission- ν followed by ^{238}U capture and ^{235}U capture, and fission cross-sections since k_{eff} is very sensitive to these reactions.

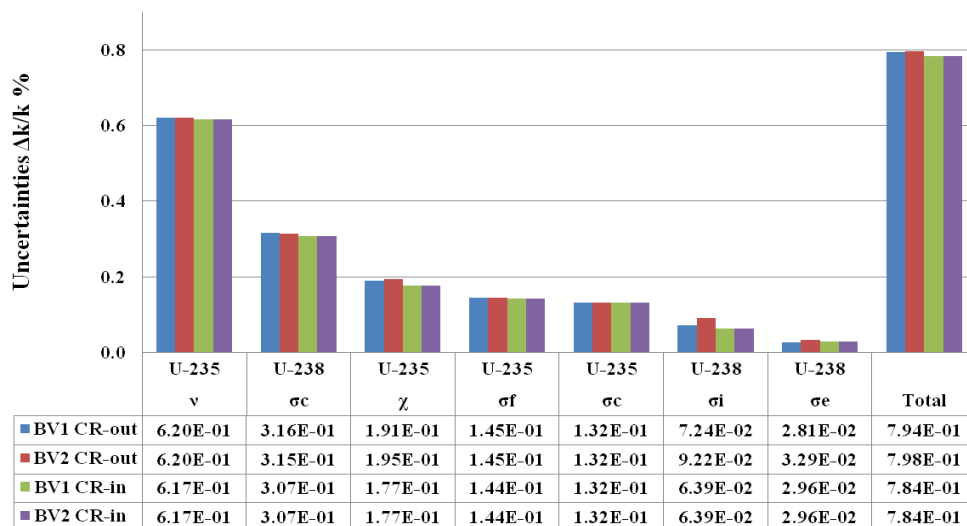


Figure 6: The Uncertainties in k_{eff} for BV1 and BV2

The ^1H elastic scattering has no contribution although its sensitivity is high (as seen in Figure 3), this is because the relative standard deviation ^1H elastic is very small. Even though the ^{235}U fission- χ sensitivity is very small, it contributes to uncertainties because it has very high standard deviations, the same for the ^{238}U elastic and inelastic scattering. The relative standard deviation for ^1H elastic, ^{235}U fission- χ , ^{238}U elastic, and inelastic scattering are illustrated in Figures 7 (a-d).

5.2 Sensitivities and Uncertainties in reactivity

Now, the influence of the modifications in the control rods designs is studied by comparing the sensitivity and uncertainty of reactivities resulting from control rods insertions. In Figure 8, the absolute value of energy-integrated sensitivity coefficients in reactivities for BV1 and BV2 models due to cross-section perturbations are explained.

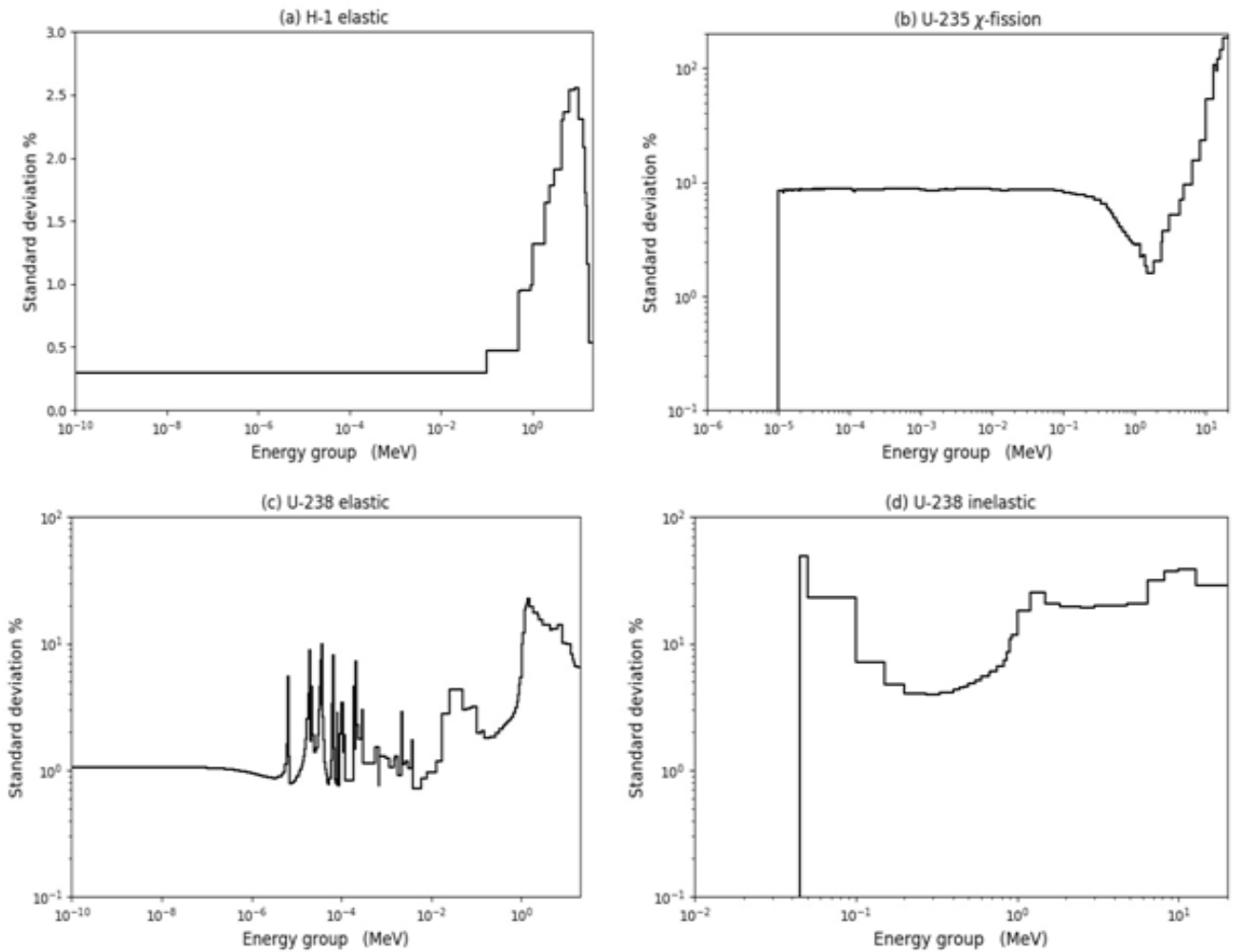


Figure 7: The relative standard deviation for ¹H elastic, ²³⁵U fission- γ , ²³⁸U elastic, and inelastic scattering

Based on Eq.(4), the sensitivities in reactivity is calculated from the differences between the k_{eff} sensitivities of the two states (control rods in and out), accordingly, the BV1 model is very sensitive to the ¹H elastic scattering cross-section as a result of the large difference in the k_{eff} sensitivities when control rods are in and out. This difference does not occur in

the BV2 model because the slight increase in ¹H scattering due to the higher coolant density in the nozzle and support plate structures partially compensated the sharp decrease due to control rods insertion.

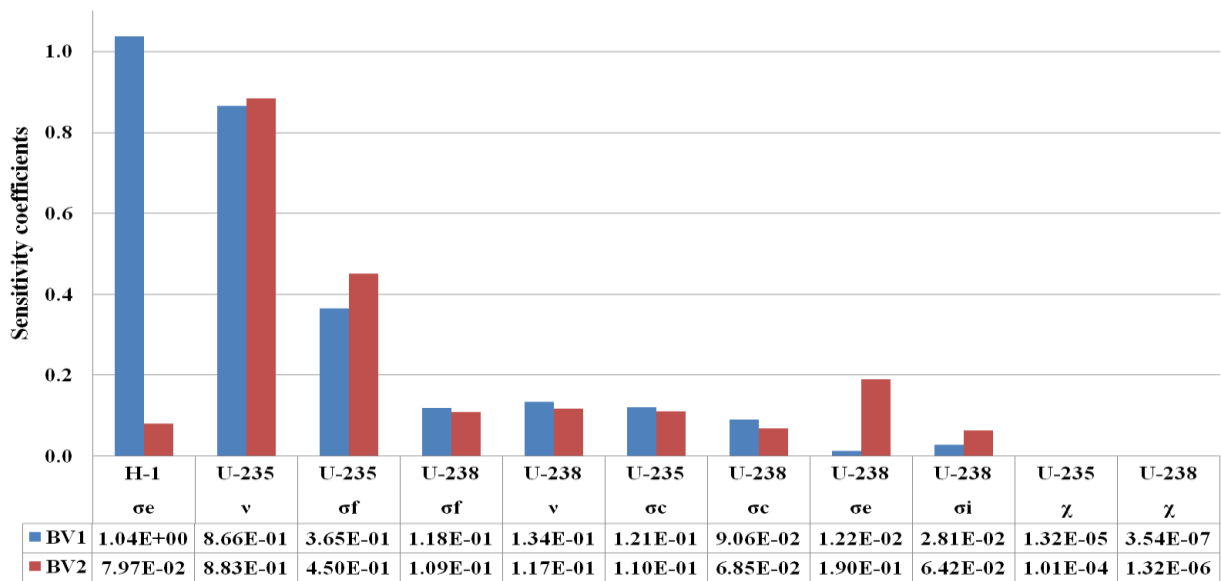


Figure 8: The integrated sensitivities in reactivities for BV1 and BV2

Some reactions, such as ^{238}U elastic and inelastic scattering, have the opposite behavior where the sensitivities in reactivities for the BV2 model are much greater than the BV1 model because of the larger differences between the k_{eff} sensitivities of the two states for BV2 model as explained before.

Figure 9 illustrates the uncertainties in reactivities due to control rods insertion for both BV1 and BV2 models. The total uncertainties in reactivities for BV2 is greater than the BV1 model, the total uncertainties are 2.28 and 1.41 $\Delta k/k$ % for BV2 and BV1, respectively. The main contributors to the

uncertainties in reactivities are the ^{238}U inelastic, elastic, ^{235}U fission- χ followed by ^{235}U fission- ν and ^{238}U fission- χ .

Although the ^{238}U inelastic, elastic, and ^{235}U fission- χ sensitivity are smaller than ^{235}U fission- ν , however, they significantly contribute to uncertainties due to the high standard deviations in their cross-sections (please refer to Figure 7) compared to ^{235}U fission- ν as shown in Figure 10.

According to Eq. (6), whenever the difference in the k_{eff} of the two states is small (control rods are out and in), the relative variance of the reactivity is substantially greater than the individual k_{eff} variances. Consequently, the relative uncertainties in reactivity responses are inherently large.

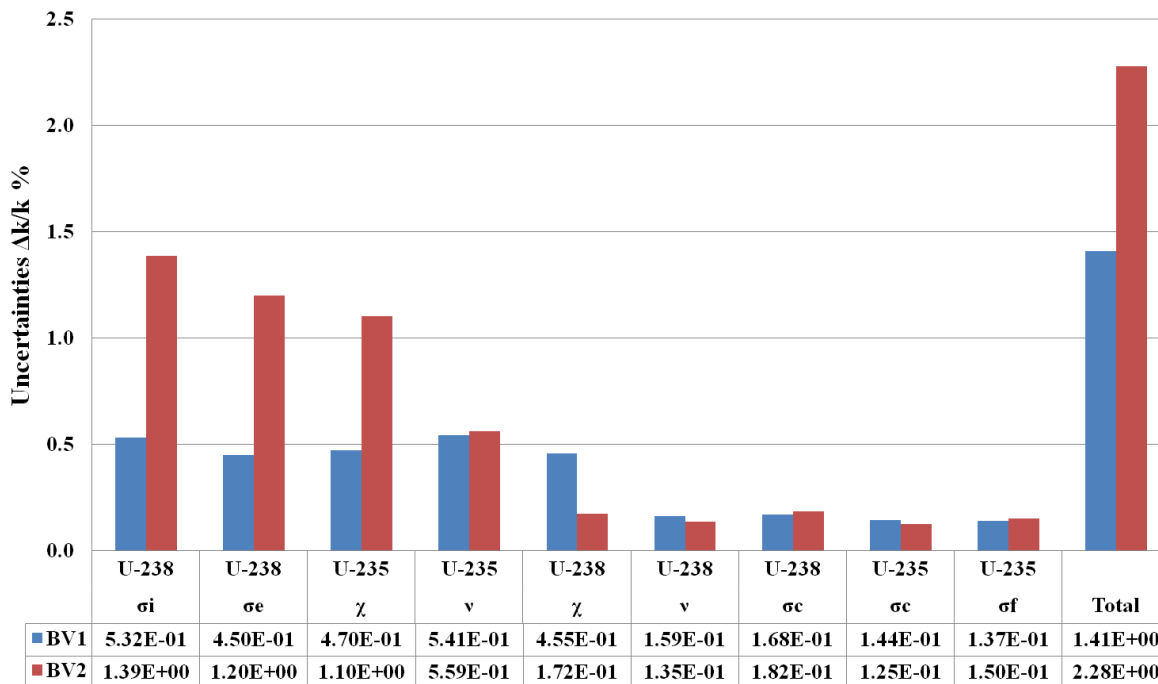


Figure 9: The Uncertainties in reactivity for BV1 and BV2

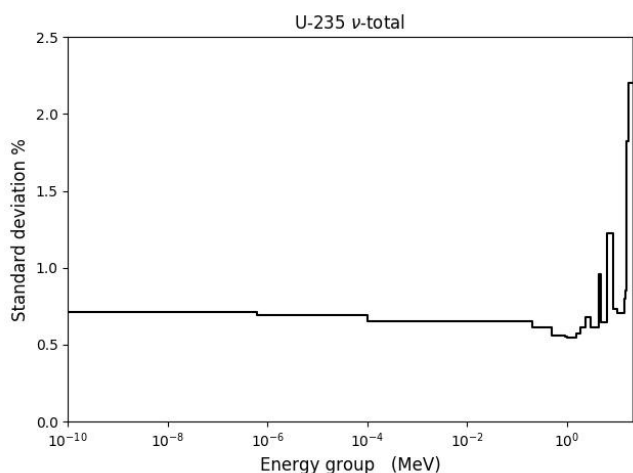


Figure 10: The relative standard deviation for U-235 fission- ν

6. Conclusions

The sensitivity and uncertainty due to model modifications in the BEAVRS benchmark were evaluated. The first and

last core designs of the benchmark were simulated using MCNP6. The sensitivity coefficient was estimated using the KSEN card that utilizes the adjoint method. NJOY2021 was used to produce the covariance matrix required to estimate uncertainty.

It was found that the modification of the upper and lower structure of BV2, as well as burnable absorber design, had a significant effect on the sensitivity of the multiplication factor. Where the multiplication factor is very sensitive to ^{235}U fission- ν , fission, and ^{238}U capture cross-sections. The main contributors to the k_{eff} uncertainties were the ^{235}U fission- ν followed by ^{238}U capture and ^{235}U capture, and fission cross-sections.

In the BV1 model, the reactivity was very sensitive to the ^1H elastic scattering cross-section as a result of the large difference in the k_{eff} sensitivities. The total uncertainties in reactivity for BV2 is 62% greater than that of the BV1 model, due to the effect of using higher coolant density in the nozzle and support plate structures in addition to the effect of the burnable absorber designs in the BV2 model. The main contributors to the uncertainties in reactivities

were the ^{238}U inelastic, elastic, ^{235}U fission- γ uncertainties due to the high standard deviations in their cross-sections.

References

- [1] D. G. Cacuci, (2003), "Sensitivity and Uncertainty Analysis", Theory, Vol. 1. Chapman & Hall/CRC, Boca Raton.
- [2] C.J. Diez, O. Buss, et al., (2015), "Comparison of nuclear data uncertainty propagation methodologies for PWR burn-up simulations", *Annals of Nuclear Energy*, 77 (101–114).
- [3] P. Reuss. (2008), "Neutron Physics". EdP Sciences, France.
- [4] MIT Computational Reactor Physics Group, (2013) "BEAVRS benchmark for evaluation and validation of reactor simulations", Rev. 1.1.1. Cambridge, UK:MIT CRPG.
- [5] MIT Computational Reactor Physics Group, (2017), "BEAVRS benchmark for evaluation and validation of reactor simulations", Rev. 2.0.1. Cambridge, UK:MIT CRPG.
- [6] MIT Computational Reactor Physics Group, (2018), "BEAVRS benchmark for evaluation and validation of reactor simulations", Rev. 2.0.2. Cambridge, UK:MIT CRPG.
- [7] D.B. Pelowitz, (2013), "MCNP6 User's Manual Version 1.0, Los Alamos National Laboratory report, LA-CP-13-00634, Rev. 0.
- [8] B.C.Kiedrowski, (2013), "MCNP6.1 k-Eigenvalue Sensitivity Capability: A User's Guide", Los Alamos National Laboratory report, LA-UR-13-22251.
- [9] R. E. MacFarlane, et. al. (2019), "The NJOY Nuclear Data Processing System, Version 2016", LA-UR-17-20093, updated October 2019. <https://www.njoy21.io/NJOY21/>.
- [10] M. L. Williams, (2007), "Sensitivity and Uncertainty Analysis for Eigenvalue-Difference Responses," *Nuclear Science and Engineering*, 155 (18–36).
- [11] Chadwick, M.B., et.al, ENDF/B-VII.1 Nuclear Data for Science and Technology: Cross Sections, Covariance, Fission Product Yields and Decay Data, (2011).